Generalized x-ray scattering cross section from nonequilibrium plasmas

G. Gregori
CCLRC, Rutherford Appleton Laboratory, Chilton, Didcot OX11 0QX, Great Britain
and Clarendon Laboratory, University of Oxford, Parks Road, Oxford, OX1 3PU, Great Britain

S. H. Glenzer and O. L. Landen
Lawrence Livermore National Laboratory, University of California, P.O. Box 808, California 94551, USA
(Received 3 May 2006; published 22 August 2006)

We propose a modified x-ray form factor that describes the scattering cross section in warm dense matter valid for both the plasma and the solid (crystalline) state. Our model accounts for the effect of lattice correlations on the electron-electron dynamic structure, as well as provides a smooth transition between the solid and the plasma scattering cross sections. In addition, we generalize the expression of the dynamic structure in the case of a two-temperature system (with different electron and ion temperatures). This work provides a unified description of the x-ray scattering processes in warm and dense matter, as the one encountered in inertial confinement fusion, laboratory astrophysics, material science, and high-energy density physics and it can be used to verify temperature relaxation mechanisms in such environments.

DOI: 10.1103/PhysRevE.74.026402 PACS number(s): 52.70.La, 71.10.Ca, 61.10.Eq, 52.38.−r

I. INTRODUCTION

X-ray scattering of solid density plasmas has been proved a successful technique for the characterization of warm and dense states of matter [1–5], as the ones created in high-energy density experiments relevant for inertial confinement fusion (ICF) [6] and found in the interior of stars and planets. It was shown that by extending the theory of spectrally resolved Thomson scattering to the hard x-ray regime, accurate measurements of the electron temperature, electron density, and ionization state can be obtained. In this respect, comparison of the experimental results with equation of state (EOS) models has revealed important insights on the microscopic state of solid density beryllium and carbon plasmas [3,4].

Those experiments were aimed to study relatively high temperature regimes, where the matter is in a plasma state. On the other hand, as the temperature is decreased and the degree of coupling between charged particles increases, a transition from a plasma to a solid state occurs. This transition involves the formation of highly ordered arrangements of the atoms (i.e., a crystal is formed) as well as an overall modification of the energy states available to the electrons. In addition to crystallization, indication of a plasma phase transition in hydrogen at $T\sim 1$ eV involving a change of its chemical composition has been discussed [7,8]. The changes in the electron binding that occurs at the onset of a phase transition are characterized by a corresponding change in the macroscopic transport properties such as electrical and thermal conductivities. On the other hand, these properties are extremely important for a correct understanding of the EOS and the optical behavior of matter found in laboratory and astrophysical environments, such as ICF, interior of planets, and high-energy density physics. Theoretical studies on the plasma to solid phase transition in a one component plasma have been presented in the context of spectroscopy of astrophysical clouds in the Galaxy [9]. These changes in both spatial arrangements and energy states also reflect a change in the way light is scattered by these systems.

In this work we provide a unified description of the x-ray scattering form factor (the dynamic structure factor), which is the fundamental quantity describing the x-ray cross section, for both nonequilibrium conditions (with separate temperatures for ions and electrons) and either at the plasma or the solid state. Our results, for example, can be applied to interpret experiments from solid density plasmas undergoing crystallization, thus providing a powerful experimental technique for the validation of EOS models in such regimes [10,11]. Time resolved diffraction experiments on liquid-to-solid phase transitions have also recently been presented [12–14]. While in those original studies work was done in the understanding of the change of the Bragg reflected light, in the present study we mainly concentrate our analysis on the scattering processes occurring outside the Bragg peaks. Finally, we provide necessary framework for the understanding of x-ray scattering experiments from shock heated matter, where strong nonequilibrium conditions may exist [15], as well as to study temperature relaxation in radiatively heated matter [16]. The paper is organized as follows: in Secs. II A and II B we introduce the basic concepts of the model; in Sec. II C we develop a two-temperature plasma model; Sec. II D is devoted to the inclusion of lattice effects while Sec. II D discusses the effect of energy bands. All of these effects are put together in Sec. III where synthetic spectra for conditions found in laser plasma experiments are constructed. A summary and concluding remarks are drawn in Sec. IV.

II. THEORY

A. Basic concepts

Following the discussion in Ref. [17], we describe the scattering from a uniform plasma containing N ions per unit volume. If Z_A is the nuclear charge of the ion, the total number of electrons per unit volume in the system, including free and bound ones, is $Z_A N$. Let us now assume we probe such a system with x rays of frequency ω_0 such that $\hbar\omega_0 \gg E_I$, with E_I the ionization energy of any bound electron, i.e., the incident frequency must be large compared to any natural absorption frequency of the scattering atom,

which allows us to neglect resonant scattering. During the scattering process, the incident photon transfers momentum $\hbar\mathbf{k}$ and energy $\hbar\omega=\hbar\omega_0-\hbar\omega_1$ to the electron, where ω_1 is the frequency of the scattered radiation, and in the nonrelativistic limit ($\hbar\omega \ll \hbar\omega_0$) accounting for refractive index change,

$$k = |\mathbf{k}| = \frac{4\pi}{\lambda_0}\sin(\theta/2)\sqrt{1-\frac{\omega_{pe}^2}{\omega_c^2}}, \tag{1}$$

with $\lambda_0=2\pi c/\omega_0$ the probe wavelength, θ the scattering angle, $\omega_{pe}=(e^2n_e/\epsilon_0 m_e)^{1/2}$ the electron plasma frequency, and $\omega_c=2\pi c/\lambda_0$ the critical frequency. Here n_e is the electron density, m_e is the electron mass, and c is the speed of light. We denote with Z_f and Z_c the number of free and bound electrons, respectively. Clearly, $Z_A=Z_f+Z_c$. Here Z_c includes both tightly bound and weakly bound electrons. These electrons are bound to a single atom. Since Z_f represents electrons which are not bound to any single atom, we will also refer to it as the number of delocalized, valence, or conduction electrons. Following the approach of Chihara [18,19] the scattering cross section is described in terms of the dynamic structure factor of all the electrons in the plasma:

$$S(k,\omega) = |f_I(k)+q(k)|^2 S_{ii}(k,\omega) + Z_f S_{ee}^0(k,\omega) + Z_c\int \tilde{S}_{ce}(k,\omega-\omega')S_s(k,\omega')d\omega'. \tag{2}$$

The first term in Eq. (2) accounts for the density correlations of electrons that dynamically follow the ion motion. This includes both the bound electrons, represented by the ion form factor $f_I(k)$, and the screening cloud of free (and valence) electrons that surround the ion, represented by $q(k)$ [1]. $S_{ii}(k,\omega)$ is the ion-ion density correlation function. The second term in Eq. (2) gives the contribution in the scattering from the free electrons that do not follow the ion motion. Here, $S_{ee}^0(k,\omega)$ is the high frequency part of the electron-electron correlation function [20] and it reduces to the usual electron feature [21,22] in the case of an optical probe. Inelastic scattering by bound electrons is included in the last term of Eq. (2), which arises from bound-free transitions to the continuum of core electrons within an ion, $\tilde{S}_{ce}(k,\omega)$, modulated by the self-motion of the ions, represented by $S_s(k,\omega)$.

We have discussed the generalization of Eq. (2) to the case of a multicomponent plasma in Ref. [5] and it will not be discussed further here.

B. Effective temperatures for electrons and ions

In the analysis we have developed in our previous work [4,17], it was assumed that the plasma is in local thermodynamic equilibrium (LTE) with the same electron and ion temperatures. While for solid density plasmas, at relatively high temperatures, the condition of LTE is closely approached due to fast relaxation between ions and electrons, at lower temperatures the concept of LTE is more subtle [23], and it is complicated by degeneracy effects. We shall treat degeneracy for electrons and ions independently due to their different thermal de Broglie wavelengths compared to the average interparticle distance. In the limit $T_e\to 0$ (T_e is the electron temperature), the electron fluid is treated using the approach suggested by Dharma-Wardana and Perrot [24] by considering a *classical* Coulomb fluid at the temperature $T_q=T_F/(1.3251-0.1779\sqrt{r_s})$, with $r_s=d/a_B$ (a_B is the Bohr radius), T_F the Fermi temperature, and $d=(3/4\pi n_e)^{1/3}$. The correlation properties are then calculated at the effective temperature $T_e'=(T_e^2+T_q^2)^{1/2}$. This approach was shown to reproduce finite-temperature static response of an electron fluid, valid for arbitrary degeneracy [25].

Similarly, as the ion temperature (T_i) is decreased, the Coulomb forces between ions become progressively dominant over their thermal motion (in other words, ion-ion coupling increases) until crystallization occurs. The ions can still oscillate around their lattice sites and the phonons are the quantum-mechanical result of this process (see, e.g., Ref. [26]). The *stiffness* of the ion lattice with respect to phonons is calculated in terms of the Debye temperature (T_D), which has been measured for most lattices, and in the case of simple metals can be obtained through the Bohm-Staver relation [27,28]

$$T_D = \frac{\hbar}{k_B}\Omega_{pi}(k), \tag{3}$$

where k_B is the Boltzmann constant and $\Omega_{pi}(k)$ is the screened ion plasma frequency. It differs from the usual ion plasma frequency ω_{pi} because it accounts for the response of the electron fluid that surrounds each ion. We thus have $\Omega_{pi}^2(k)=\omega_{pi}^2/(1+k_{De}^2/k^2)$, where $\omega_{pi}=(Z_f e^2 n_e/\epsilon_0 m_i)^{1/2}$ with m_i the ion mass, and $k_{De}=(n_e e^2/\epsilon_0 k_B T_e')^{1/2}$ is the Debye wave number for the electron fluid. Since, in the Debye model, phonon modes with wavelength up to a fraction of the lattice spacing are considered, we set in Eq. (3) $k\equiv k_{max}=(2/Z_f)^{1/3}k_F=(6\pi^2 n_e/Z_f)^{1/3}$, where k_F is the Fermi wave number. By analogy with the electron fluid, we can define an effective temperature for the ions: $T_i'=(T_i^2+\gamma_0 T_D^2)^{1/2}$ ($\gamma_0=3/2\pi^2=0.152$), which accounts for ion degeneracy (i.e., phonon coupling) at low temperatures. This definition preserves the correct quantum-mechanical limit for the harmonic vibrations of a perfect crystal as $T_i\to 0$ [29]. Similarly, the Debye wave number for the ions can be defined as $k_{Di}=(Z_f n_e e^2/\epsilon_0 k_B T_i')^{1/2}$.

For typical conditions found in laser plasma experiments with solid density beryllium [3], we have $n_e\sim 2.5\times 10^{23}$ cm^{-3} and $Z_f\sim 2$. This gives $T_F\sim 14.5$ eV and $T_D\sim 0.16$ eV. Thus degeneracy effects become important for the electrons when $T_e\lesssim T_F=14.5$ and ion lattice effects must be considered when $T_i\lesssim T_D=0.16$ eV.

C. Scattering form factor from a nonequilibrium plasma

Within the framework of the density response formalism for a two component plasma, we can calculate the screened interaction potentials using the semiclassical approach suggested by Arkhipov and Davletov [30], which is based on a pseudopotential model for the interaction between charged

particles to account for quantum diffraction effects (i.e., the Pauli exclusion principle) and symmetry [31–33]. Quantum diffraction is represented by the thermal de Broglie wavelength $\lambda_{rs}=\hbar/(2\pi\mu_{rs}k_BT'_{rs})^{1/2}$ with $\mu_{rs}=m_rm_s/(m_r+m_s)$ the reduced mass of the interacting pair, and $r,s=e$ (electrons) or i (ions). The effective temperature T'_{rs} is given by [34],

$$T'_{rs}=\frac{m_rT'_s+m_sT'_r}{m_r+m_s}. \tag{4}$$

Due to the large mass difference between ions and electrons, $T'_{ei}\approx T'_{ee}$.

In LTE, the fluctuation-dissipation theorem (see, e.g., Ref. [35]) can be used to correlate the dielectric response of the medium and the corresponding electron density fluctuation spectrum. In other terms, a simple relation exists between the screened interaction potentials, $\Phi_{rs}(k)$, and the static response of the medium, $S_{rs}(k)$. As the system departs from LTE, the validity of the fluctuation-dissipation theorem may be questionable [36]. On the other hand, as shown in Ref. [37] the fluctuation-dissipation theorem may be still a valid approximation even under nonequilibrium conditions if the temperature relaxation is slow compared to the electron density fluctuation time scale. A common condition in experimental plasmas for this to occur is when $m_i\gg m_e$ so that the coupling between the two components takes place at sufficiently low frequency. Using a two-component hypernetted-chain (HNC) approximation scheme, Seuferling *et al.* [34] have shown that the static response under non-LTE takes the form

$$S_{rs}(k)=\delta_{rs}-\frac{\sqrt{n_rn_s}}{k_BT'_{rs}}\Phi_{rs}(k)-\delta_{er}\delta_{es}\left(\frac{T'_e}{T'_i}-1\right)\frac{|q(k)|^2}{Z_f}S_{ii}(k), \tag{5}$$

with the screening charge given by [18] $q(k)=\sqrt{Z_f}S_{ei}(k)/S_{ii}(k)$. The screened potentials $\Phi_{rs}(k)$ are given explicitly in the Appendix. Having developed this formalism, we are now able to evaluate all terms in Eq. (2) for a non-LTE plasma. Symmetry in the electron-ion interactions requires $S_{ei}(k)=S_{ie}(k)$. Since the ion motion will exhibit long-time fluctuations at the ion plasma frequency and/or sound speed, and the frequency scale of those fluctuations is such that we are currently unable to experimentally resolve them, it is reasonable to assume in Eq. (2) $S_{ii}(k,\omega)=S_{ii}(k)\delta(\omega)$. The measured width of the feature is thus solely determined by the instrument resolution. The ionic form factor $f_I(k)$ is related to the spatial distribution of electrons that are *truly* bound to the ions, and it can be calculated, for example, following the approach described in Pauling and Sherman [4,38].

For the high-frequency electron density fluctuations, we can again use the fluctuation-dissipation theorem and set the high frequency dielectric response in the random phase approximation (RPA) [39,40],

$$S^0_{ee}(k,\omega)=-\frac{\hbar}{1-\exp(-\hbar\omega/k_BT_e)}\frac{\epsilon_0k^2}{\pi e^2n_e}\mathrm{Im}\left[\frac{1}{\epsilon(k,\omega)}\right], \tag{6}$$

with $\epsilon(k,\omega)\equiv\epsilon_{RPA}(k,\omega)=1-v(k)\chi_0(k,\omega)$, where $v(k)=e^2/\epsilon_0k^2$ is the Fourier transform of the bare Coulomb potential and $\chi_0(k,\omega)$ is the density response of the noninteracting electron system. Local field corrections to the RPA in the x-ray scattering context have been discussed previously [41–43]. However, we should point out that for many plasma conditions found in laser plasma experiments, such corrections are marginal. For example, let us consider the case of a solid density beryllium plasma with $n_e\sim2.5\times10^{23}$ cm^{-3} and $T_e=20$ eV, the electron-electron coupling constant $\Gamma_{ee}=e^2/(4\pi\epsilon_0k_BT'_ed)\sim0.6$, thus the degree of coupling is still quite modest. Equation (6) explicitly includes detailed balance: $S^0_{ee}(k,\omega)=\exp(-\hbar\omega/k_BT_e)S^0_{ee}(k,-\omega)$. In other terms, as $T_e\to0$, excitations that result in an energy gain for the photons are suppressed. This is a statistical effect that originates in the quantum-mechanical nature of the electron fluid at low temperature, i.e., in the ground state, electrons cannot lower their energy anymore. We should notice that detailed balance gives a direct measure of the kinetic electron temperature (T_e), independent of the details of the microscopic theory, provided that both the red and blue components of the structure factor $S^0_{ee}(k,\omega)$ can be measured. This is the case when $\hbar\omega_{pe}\sim k_BT_e$, and for solid density beryllium this occurs at $T_e\sim20$ eV.

Finally, the calculation of the last term in Eq. (2) can be easily done within the impulse approximation scheme, as discussed in Ref. [4]. This concludes the required formalism to analytically construct the x-ray scattering spectrum from a dense plasma which is far from LTE conditions.

We shall now investigate the effects of non-LTE in the scattering spectrum. Let us consider again the case of a dense beryllium plasma with $n_e\sim2.5\times10^{23}$ cm^{-3}, $Z_f=2$, and $T_e=20$ eV. In Fig. 1 we have plotted the static structures $S_{rs}(k)$ and the screening charge $q(k)$ for different values for the ratio T_i/T_e. We see that consistent differences between the equilibrium values and the non-LTE ones, especially for the ion-ion structure factor, are found up to $k/k_{De}\lesssim15$ (or $\alpha=k_{De}/k\gtrsim0.07$). This would correspond to an x-ray probe with energy $\lesssim30$ keV for a 90° scattering angle. On the

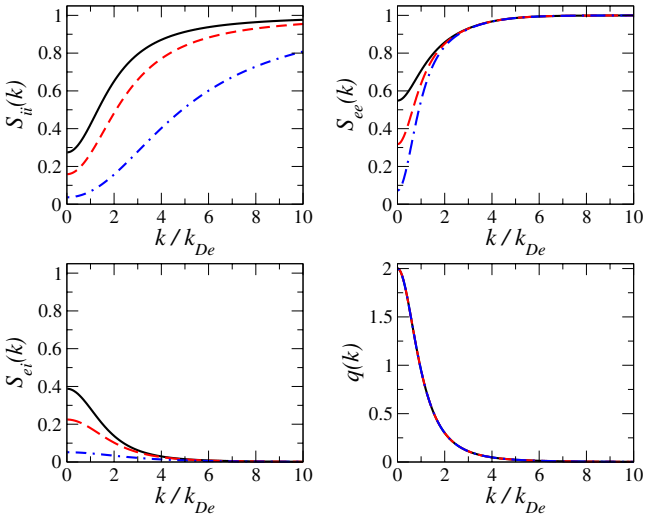

FIG. 1. (Color online) Calculated structure factors $S_{rs}(k)$ and screening charge $q(k)$ for a beryllium plasma with $n_e\sim2.5\times10^{23}$ cm^{-3}, $Z_f=2$, and $T_e=20$ eV. $T_i/T_e=1$ (solid line), $T_i/T_e=0.5$ (dashed line), and $T_i/T_e=0.1$ (dashed-dotted line).

other hand, as the screening distance is mainly determined by the more mobile electrons, $q(k)$ remains independent on the changes of the ion temperature. The electron-electron static structure is related to the ion-ion structure by the relation [19] $S_{ee}(k)=[|q(k)|^2/Z_f]S_{ii}(k)+S^0_{ee}(k)$, where $S^0_{ee}(k)$ is the static response associated to the highly mobile electrons. Note that the screening charge $q(k)$ has been constructed such that, in the Debye-Hückel limit, $S^0_{ee}(k)$ is also independent on T_i. We should recall that the suppression of the ion response in a classical plasma has been discussed by Kunze [44] in the context of optical Thomson scattering.

At sufficiently low probe energies, the LTE assumption overestimates the intensity of the elastic scattering when the system departs from equilibrium conditions. In the regime where $k \gtrsim k_{De}$ (i.e., noncollective scattering), the elastic component in the scattering spectrum can be approximated as [17]

$$I_i = Z_c^2 S_{ii}(k), \tag{7}$$

where Z_c is strictly the number of tightly bound (K-shell) electrons for which their ionization energy is much larger than the Compton recoil. We see that an overestimate of S_{ii} corresponds to an underestimate of Z_c, with $|\Delta Z_c/Z_c|=|\Delta S_{ii}/2S_{ii}|$. Attention should then be applied in the analysis of experimental spectra for the measurement of the average ionization state, as errors in Z_c (or Z_f) up to $\sim$30% are possible if strong non-LTE conditions are present. On the other hand, we should point out that the model implemented for the calculation of $S_{ii}(k)$ is based on a variation of the RPA and thus its applicability at large ion coupling may miss the formation of long-range ordering of the ions (i.e., a lattice). We will incorporate such effects with the analysis developed in the next section.

D. Lattice effects

As the ion temperature is reduced, the Coulomb interaction between ions start to dominate over their kinetic energy. The degree of ion coupling is expressed by the parameter $\Gamma_{ii}=Z_f^2e^2/4\pi\epsilon_0 k_B T_i' d_{ii}$, where $d_{ii}=(3Z_f/4\pi n_e)^{1/3}$ is the mean ionic separation (or Wigner-Seitz cell). The ion-ion coupling parameter is related to the electron-electron coupling parameter by the relation $\Gamma_{ii}=Z_f^{5/3}(T_e'/T_i')\Gamma_{ee}$, thus for most experimental conditions, the electrons remain weakly coupled even if the ions are strongly coupled. The analysis we have carried on so far does not include direct effects in the scattering which are associated with the underlying lattice arrangements. The most predominant of such modifications in the scattering cross section (2) is in the appearance of Bragg diffraction. As discussed in Ref. [45] the continuity of the structure factors across the phase boundary is necessary in order to preserve the thermodynamic and transport properties of the medium. Let us consider a generalized version of Eq. (2):

$$S(k,\omega) = |f_I(k) + q(k)|^2 S_{II}(k,\omega) + Z_f S^0_{EE}(k,\omega) + Z_c \int \tilde{S}_{ce}(k,\omega-\omega')S_s(k,\omega')d\omega', \tag{8}$$

where here $S_{II}(k,\omega)$ and $S^0_{EE}(k,\omega)$ simply denotes a more general form for the ion-ion and free electron structure factors (the core electron structure factor instead does not depend on the thermodynamic status of the medium, but only on the core atomic structure of the ion which we regard to remain unaffected by such changes). The most general definition of the ion-ion structure factor is [19]

$$S_{II}(k,\omega) = \frac{1}{2\pi N}\int \sum_r \langle e^{i\mathbf{k}\cdot[\mathbf{R}_r(t)-\mathbf{R}_0(0)]}\rangle e^{i\omega t}dt, \tag{9}$$

where $\langle\cdots\rangle$ denotes a thermal average and $\mathbf{R}_r(t)$ is the position vector for the rth ion. The task in evaluating $S_{II}(k,\omega)$ is thus reduced to the calculation of

$$\mathcal{I} = \sum_r \langle e^{i\mathbf{k}\cdot[\mathbf{R}_r(t)-\mathbf{R}_0(0)]}\rangle. \tag{10}$$

Suppose that at $t=-\infty$ each atom is at the position $\mathbf{R}_r(-\infty)=\mathbf{U}_r$. Without loss of generality, we can pick $t=-\infty$ as the time when the system was in the cold solid state. In this case, the vectors $\mathbf{U}_r$ give the position of each atom in the initial lattice. We then decompose the motion of each ion as the sum of two distinct terms: an oscillation (vibration), $\mathbf{u}_r(t)$, around the instantaneous center of mass of each atom, and a global translation of the centers of mass, $\mathbf{x}_r(t)$. Clearly, we must have $\mathbf{R}_r(t)=\mathbf{U}_r+\mathbf{u}_r(t)+\mathbf{x}_r(t)$, with the condition $\langle\mathbf{u}_r(t)\rangle=0$. With this is mind, we can rewrite Eq. (10) as

$$\mathcal{I} = \sum_r e^{i\mathbf{k}\cdot(\mathbf{U}_r-\mathbf{U}_0)}\langle e^{i\mathbf{k}\cdot[\mathbf{u}_r(t)-\mathbf{u}_0(0)]}e^{i\mathbf{k}\cdot[\mathbf{x}_r(t)-\mathbf{x}_0(0)]}\rangle. \tag{11}$$

Let also assume that the lattice vibrations $\mathbf{u}_r(t)$ and the site translations $\mathbf{x}_r(t)$ are statistically independent. We should note that this assumption may not hold if, for example, intense external fields are applied to the system. This implies

$$\langle e^{i\mathbf{k}\cdot[\mathbf{u}_r(t)-\mathbf{u}_0]}e^{i\mathbf{k}\cdot[\mathbf{x}_s(t)-\mathbf{x}_0]}\rangle = \delta_{rs}\langle e^{i\mathbf{k}\cdot[\mathbf{u}_r(t)-\mathbf{u}_0]}\rangle\langle e^{i\mathbf{k}\cdot[\mathbf{x}_s(t)-\mathbf{x}_0]}\rangle, \tag{12}$$

where we have used the shorthand notation $\mathbf{u}_0(0)\equiv\mathbf{u}_0$ and $\mathbf{x}_0(0)\equiv\mathbf{x}_0$. Under these conditions

$$\mathcal{I} = \left(\sum_r \langle e^{\mathbf{k}\cdot[\mathbf{x}_r(t)-\mathbf{x}_0]}\rangle\right)\times\left(\sum_r e^{i\mathbf{k}\cdot(\mathbf{U}_r-\mathbf{U}_0)}\langle e^{\mathbf{k}\cdot[\mathbf{u}_r(t)-\mathbf{u}_0]}\rangle\right). \tag{13}$$

The second part of the previous expression containing the thermal average of the lattice vibrations can be treated using the Debye model in the zero-phonon approximation, as described, for example, by Warren [46]. Using the fact that, for any variable u, $\langle e^u\rangle=e^{\langle u^2\rangle/2}$, we have

$$\sum_r e^{i\mathbf{k}\cdot(\mathbf{U}_r-\mathbf{U}_0)}\langle e^{\mathbf{k}\cdot[\mathbf{u}_r(t)-\mathbf{u}_0]}\rangle = (1-e^{-2W}) + e^{-2W}b(k), \tag{14}$$

where

$$b(k) = \frac{1}{N}\sum_{r,s} e^{i\mathbf{k}\cdot(\mathbf{U}_r-\mathbf{U}_s)} \tag{15}$$

is the Bragg peak, and

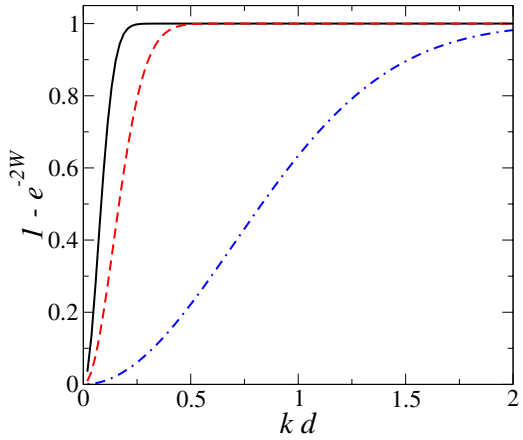

FIG. 2. (Color online) Calculated Debye-Waller correction factors for solid beryllium with $n_e \sim 2.5\times 10^{23}$ cm^{-3}, $Z_f=2$, and $T_e=20$ eV. $T_i/T_e=1$ (solid line), $T_i/T_e=0.5$ (dashed line), and $T_i/T_e=0.1$ (dashed-dotted line). In the plot, a value of unity corresponds to no correction.

$$2W = \frac{\pi^2 k^2 \hbar^2}{4Mk_B T_D}\left(\frac{T_i'}{T_D}\right)^2 \tag{16}$$

is the Debye-Waller factor [29,46], which we have defined in terms of the effective ion temperature T_i'. This definition preserves the correct quantum-mechanical limit for $T_i \to 0$ [29]. We notice that, as T_i increases, the Debye-Waller factor gets larger and thus acts to reduce Bragg diffraction. In a high temperature plasma we expect $e^{-2W} \approx 0$ so any Bragg scattering, $b(k)$, is suppressed. This *thermal* damping of Bragg scattering is also known in the x-ray diffraction community as thermal diffuse scattering [46]. The factor $1-e^{-2W}$ for the beryllium case is plotted in Fig. 2. We clearly see that for $kd \gtrsim 0.5$ ($\alpha \lesssim 4$) the Debye-Waller factor becomes important only for $T_i/T_e \lesssim 0.5$.

In the limit of $T_i \gg T_D$, $W \to \infty$ and Eq. (13) reduces to

$$\mathcal{I} = \sum_r \langle e^{\mathbf{k}\cdot[\mathbf{x}_r(t)-\mathbf{x}_0]}\rangle, \tag{17}$$

and it becomes naturally associated to the plasma ion-ion structure factor:

$$S_{ii}(k,\omega) = \frac{1}{2\pi N}\int \sum_r \langle e^{\mathbf{k}\cdot[\mathbf{x}_r(t)-\mathbf{x}_0]}\rangle e^{i\omega t} dt. \tag{18}$$

In other terms, the plasma ion-ion structure factor is related to the response of medium to random (or thermal) fluctuations. We will calculate this term using the methods described in the previous section for a non-LTE plasma. The generalized ion-ion structure factor can be thus written as

$$S_{II}(k,\omega) = S_{ii}(k,\omega)[(1-e^{-2W}) + e^{-2W} b(k)]. \tag{19}$$

E. Simplified band structure

Another important effect which is associated with the formation of a lattice structure is the modification of the energy states available to the electrons, namely energy bands are created. In the case of electrons in the conduction band of a metal, RPA is often adequate to describe their response [39,40]. Instead, for insulators and semiconductors corrections to the RPA may be necessary. For large k scattering, electrons in either conduction or valence bands can still be considered nearly as free for x-ray scattering due to the large energy transfer with respect to the energy in the band. On the other hand, for small k scattering we can have energy gaps of the order of $\sim 10\%$ of the plasmon excitations and in this case corrections to the RPA can be important. Since we are still dealing with large excitations compared to most band gaps, we assume a model insulator (or semiconductor) with only one energy gap in the excitation spectrum. As discussed by Levine and Louie [47], the effect of such a gap is to modify the dielectric response for all frequencies above the gap and suppressing the response below it. They developed a model dielectric function at $T_e=0$ which fully preserves particle conservation (i.e., the f-sum rule). Adapting their model to finite temperatures, we have for $|\omega| \geq \omega_g$

$$\epsilon_{EE}(k,\omega) = \epsilon_{RPA}(k, \mathrm{sgn}(\omega)\sqrt{\omega^2 - \omega_g^2}), \tag{20}$$

where $\omega_g \approx E_g \exp(-k_B T_e/E_g)/\hbar$ is the excitation frequency for an energy gap E_g. For $|\omega| < \omega_g$ we instead have $\mathrm{Im}\,\epsilon_{EE}(k,\omega)=0$. The resultant form for the free electron dynamic structure is thus

$$S^0_{EE}(k,\omega) = -\frac{\hbar}{1-\exp(-\hbar\omega/k_B T_e)}\frac{\epsilon_0 k^2}{\pi e^2 n_e} \times \mathrm{Im}\left[\frac{1}{\epsilon_{EE}(k,\omega)}\right]. \tag{21}$$

Since the antisymmetry of the imaginary part of the dielectric function is maintained in this formulation, the detailed balance relation can again be implemented as a possible temperature diagnostic. Suppose we probe this model semiconductor (or insulator) with Cl Ly-α x rays of energy 2.96 keV at a scattering angle of 45°. We assume $T_F=12.5$ eV ($n_e=2\times 10^{23}$ cm^{-3}) and $T_e=10$ eV with different values for the band gap. These scattering conditions give for the scattering parameter [2] $\alpha=\omega_{pe}/kv_{te}=1.3$ ($v_{te}^2=k_B T_e'/m_e$) and $kd=1.1$, which denotes the photons being scattered by the collective response of the medium (i.e., by plasmons). The calculated structure factor $S^0_{EE}(k,\omega)$ is shown in Fig. 3. We see that the main effect of an energy band gap is to suppress excitations near $\omega=0$. Effectively, this also means that the total (nearly) elastically scattered measured signal is reduced if a band gap is present. Wecan estimate this correction in the small k case (and by assuming $T_e \sim T_i \gg T_D$ such that the non-LTE and Debye-Waller corrections are negligible). Since in this case, $f_I(k)+q(k) \approx Z_A$ [17] and the elastic scatter contribution from the ionic part is

$$I_i \approx Z_A^2 S_{ii}(k). \tag{22}$$

On the other hand, the inelastically scattered signal from free electrons near $\omega=0$ is

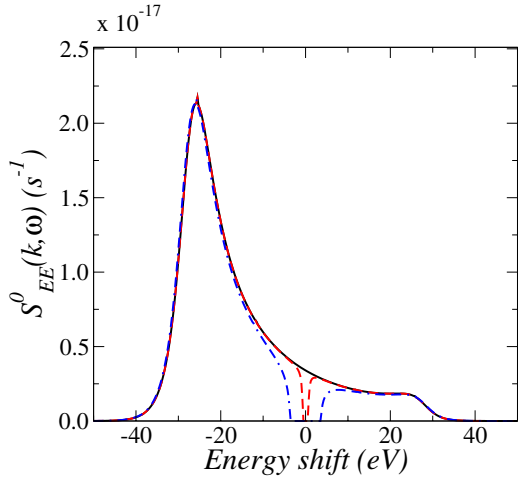

FIG. 3. (Color online) Calculated free (valence) electron dynamic structure factor for the model semiconductor (insulator) described in the text. The system is probed with x rays of energy 2.96 keV at a scattering angle of 45° with $T_F=12.5$ eV and $T_e=10$ eV. $E_g=0$ (solid line), $E_g=5$ eV (dashed line), and $E_g=10$ eV (dashed-dotted line).

$$I_e^0 \sim Z_f \omega_g S_{ee}^0(k,0) \approx \frac{\sqrt{\pi} Z_f \alpha}{2} \frac{\omega_g}{\omega_{pe}}. \tag{23}$$

Clearly, the effect of the band gap suppression in the elastically scattered radiation will be important when, say $I_e^0/I_i \gtrsim 0.1$, or

$$\alpha \gtrsim 0.06 \frac{Z_A^2 S_{ii}(k) \omega_{pe}}{Z_f \omega_g}. \tag{24}$$

We have $S_{ii} \sim 0.1-0.4$ for $\alpha > 1$ depending on the degree of nonequilibrium. Let us consider, for example, silicon at solid density with $\hbar\omega_{pe} \sim 15$ eV, $\hbar\omega_g \sim 5$ eV, and $Z_f=4$, thus Eq. (24) becomes $\alpha \gtrsim 1.5-6$. It is therefore important to include energy band corrections in the case of highly collective scattering. On the other hand, a similar calculation for the large k case (which corresponds to the noncollective scattering regime, or $\alpha \ll 1$) yields a negligible effect of the band gap in the scattering spectrum.

III. DISCUSSION AND SYNTHETIC SPECTRA

The analysis developed in the previous section shows that strong suppression of the elastically scattered light occurs for both non-LTE conditions and in the presence of a crystalline solid outside the Bragg condition. While the first effect is essentially classical [44], the second one relates to strong ion coupling. Since in a solid plasma non-LTE is associated to a cold ionic fluid, while the electron energy remains sufficiently high at the Fermi level, we should expect two temperature effects and possible suppression of elastically scattered light also when $\Gamma_{ii} \gtrsim 1$. On the other hand, lattice effects become important only at a significantly larger coupling when solidification occurs and Bragg scattering must be considered together with the possible appearance of band levels. This roughly happens when $2W \lesssim 1$. In Fig. 4 we have identified these different regimes for the case of solid density

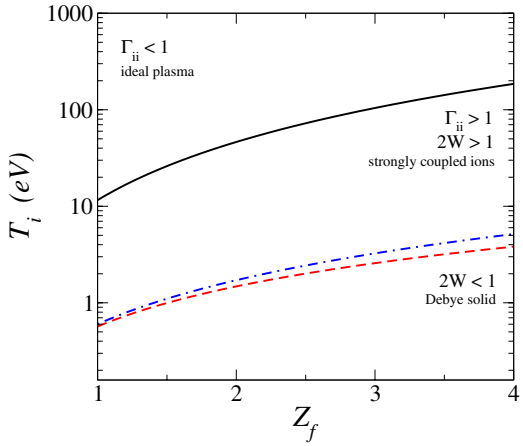

FIG. 4. (Color online) $Z_f - T_i$ diagram showing different scattering regimes for solid density beryllium. $\Gamma_{ii}=1$ (solid line), $2W=1$ for $T_i/T_e=1$ (dashed line), and $T_i/T_e=0.1$ (dashed-dotted line).

beryllium. It is clear that (for $Z_f \sim 2$) strong ion coupling becomes significant for $T_i \lesssim 10$ eV and lattice effects should be included for $T_i \lesssim 1$ eV. We need to stress that for $Z_f < 1$ the definition of the coupling parameter should also take into consideration the effect of neutral collisions. On the other hand, as $Z_f \lesssim 1$ we expect that the correlations between charged particles will be modest. Under such conditions, ion-neutral and electron-neutral collisions only marginally affect the structure factors [48].

The generalized x-ray cross section is obtained by putting Eqs. (19) and (21) into Eq. (8). In the case when the scattering angle is chosen that such eventual Bragg peaks will lie outside the detector field of view, we have for the overall dynamic structure:

$$S(k,\omega) = |f_I(k) + q(k)|^2 (1 - e^{-2W}) S_{ii}(k,\omega) + Z_f S_{EE}^0(k,\omega) + Z_c \int \tilde{S}_{ce}(k, \omega - \omega') S_s(k,\omega') d\omega'. \tag{25}$$

This expression includes the effects of both non-LTE as well as lattice dynamics. The importance of such a treatment is clearly illustrated in Fig. 5, where we have calculated the expected signal for a beryllium plasma in the case of Cl Ly-α probe x rays at 45° scattering angle. We assume $n_e \sim 2.5 \times 10^{23}$ cm^{-3}, $Z_f=2$, and $T_e=20$ eV with different values for the ion temperature. We should note that in this geometry the closest Bragg diffraction peaks occur at 35.8° and 66.4° for polycrystalline beryllium. Synthetic spectra have been generated by assuming 7 eV full width at half maximum Gaussian instrument response. As the degree of nonequilibrium is increased, there is a dramatic drop in the intensity of the elastic component. The main drop in elastic component in Fig. 5 is mainly due to nonequilibrium and only a small part (~25%) due to the density effect (i.e., Debye-Waller factor) even for the $T_i/T_e=0.1$ case. Measurement of this drop could indeed provide a novel non-LTE diagnostic of solid density plasmas.

We envision this technique as a primary diagnostic for the investigation of phase transitions in strongly coupled systems. In particular, measurement of the scattering spectrum

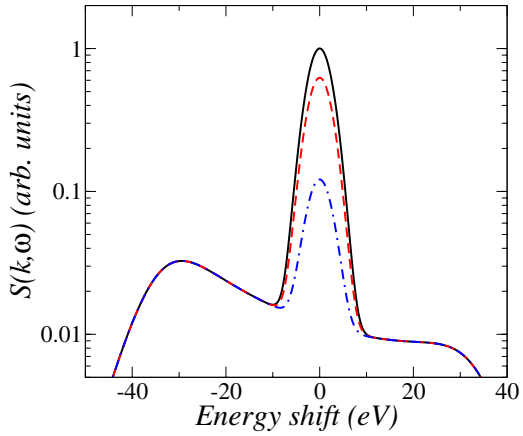

FIG. 5. (Color online) Synthetic scattering profiles for solid beryllium with $n_e \sim 2.5\times 10^{23}$ cm^{-3}, $Z_f=2$, and $T_e=20$ eV. The x-ray probe energy is 2.96 keV and the scattering angle is $\theta=45°$ (corresponding to $kd=1.1$ or $k/k_{De}=0.8$). A 7-eV full width at half maximum instrument function is assumed. $T_i/T_e=1$ (solid line), $T_i/T_e=0.5$ (dashed line), and $T_i/T_e=0.1$ (dashed-dotted line).

in shocked hydrogen could directly probe the existence of the plasma phase transition [7,8], which has been theoretically predicted as first-order phase transition between a weakly and a strongly ionized state. In this respect, the crossing of the phase boundary far from the critical point should correspond in the scattering spectrum as a change in the intensity of plasmon resonances (due to a change in Z_f). On the other hand, near the critical point, a sharp increase in the scattering cross section in the long wavelength limit is expected to occur due to the appearance of macroscopic fluctuations in the sample [49]. Clearly, the model we have presented loses its validity near the critical point.

IV. SUMMARY

This concludes our effort in treating the transition from a plasma to a solid using a common theoretical framework. The possibility for a direct investigation of nonequilibrium solid density matter undergoing phase transitions is of extreme interest for the understanding of the EOS for conditions relevant for laboratory astrophysics as well as for the characterization of shock heated materials in ICF experiments. This work provides the necessary background for implementing x-ray scattering as such diagnostics. The only free parameters in the problem are the ion and electron temperatures and their respective densities. The x-ray response of the medium as a function of these parameters is then obtained from general concepts. Some limitations of the model should be, however, kept in mind. In the analysis of the solid x-ray scattering response, for example, we have limited ourselves to a very simple picture of a lattice and neglected any possible anisotropies as well as we have not considered more than a single atom in the lattice cell. We believe that these approximations are sufficient to treat simple metals and plasmas undergoing crystallization, but a more accurate treatment may be required for complex systems. We leave this to a future work.

ACKNOWLEDGMENTS

The work of S.H.G. and O.L.L. was performed under the auspices of the U.S. Department of Energy by the University of California Lawrence Livermore National Laboratory under Contract No. W-7405-ENG-48 and by LDRD Grant No. 05-ERI-003. The work of G.G. was supported by the Council for the Central Laboratory of the Research Councils (UK).

APPENDIX

The screened potential $\Phi_{rs}(k)$ appearing in Eq. (5) are given by [17,30]

$$\Phi_{ee}(k)=\frac{e^2}{\epsilon_0\Delta}\left[\frac{k^2}{1+k^2\lambda_{ee}^2}+k_{Di}^2\left(\frac{1}{(1+k^2\lambda_{ee}^2)(1+k^2\lambda_{ii}^2)}-\frac{1}{(1+k^2\lambda_{ei}^2)^2}\right)+A\left(k^2+\frac{k_{Di}^2}{1+k^2\lambda_{ii}^2}\right)k^2\exp(-k^2/4b)\right], \tag{A1}$$

$$\Phi_{ii}(k)=\frac{Z_f^2e^2}{\epsilon_0\Delta}\left[\frac{k^2}{1+k^2\lambda_{ii}^2}+k_{De}^2\left(\frac{1}{(1+k^2\lambda_{ee}^2)(1+k^2\lambda_{ii}^2)}-\frac{1}{(1+k^2\lambda_{ei}^2)^2}\right)+\frac{Ak^2k_{De}^2}{1+k^2\lambda_{ii}^2}\exp(-k^2/4b)\right], \tag{A2}$$

$$\Phi_{ei}(k)=-\frac{Z_fe^2}{\epsilon_0\Delta}\frac{k^2}{1+k^2\lambda_{ei}^2}, \tag{A3}$$

where $b=(\lambda_{ee}^2\pi\ln 2)^{-1}$, $A=k_BT'_{ee}\ln 2\pi^{3/2}b^{-3/2}\epsilon_0/e^2$, and

$$\Delta=k^4+\frac{k^2k_{De}^2}{1+k^2\lambda_{ee}^2}+\frac{k^2k_{Di}^2}{1+k^2\lambda_{ii}^2}+k_{De}^2k_{Di}^2\left(\frac{1}{(1+k^2\lambda_{ee}^2)(1+k^2\lambda_{ii}^2)}-\frac{1}{(1+k^2\lambda_{ei}^2)^2}\right)+Ak^2k_{De}^2\left(k^2+\frac{k_{Di}^2}{1+k^2\lambda_{ii}^2}\right)\exp(-k^2/4b). \tag{A4}$$

The inverse of the electron and the ion Debye lengths are $k_{De}=(n_ee^2/\epsilon_0k_BT'_{ee})^{1/2}$ and $k_{Di}=(Z_fn_ee^2/\epsilon_0k_BT'_{ii})^{1/2}$, respectively. In Eqs. (A1)–(A4) the thermal de Broglie wavelength is defined by $\lambda_{rs}=\hbar/(2\pi\mu_{rs}k_BT'_{rs})^{1/2}$ with $\mu_{rs}=m_rm_s/(m_r+m_s)$ the reduced mass of the interacting pair.

[1] D. Riley, N. C. Woolsey, D. McSherry, I. Weaver, A. Djaoui, and E. Nardi, Phys. Rev. Lett. **84**, 1704 (2000).
[2] O. L. Landen, S. H. Glenzer, M. J. Edwards, R. W. Lee, G. W. Collins, R. C. Cauble, W. W. Hsing, and B. A. Hammel, J. Quant. Spectrosc. Radiat. Transf. **71**, 465 (2001).
[3] S. H. Glenzer, G. Gregori, R. W. Lee, F. J. Rogers, S. W. Pollaine, and O. L. Landen, Phys. Rev. Lett. **90**, 175002 (2003).
[4] G. Gregori, S. H. Glenzer, F. J. Rogers, S. M. Pollaine, O. L. Landen, C. Blancard, G. Faussurier, P. Renaudin, S. Kuhlbrodt, and R. Redmer, Phys. Plasmas **11**, 2754 (2004).
[5] G. Gregori *et al.*, J. Quant. Spectrosc. Radiat. Transf. **99**, 225 (2006).
[6] J. D. Lindl, *Inertial Confinement Fusion* (Springer-Verlag, New York, 1998).
[7] D. Beule *et al.*, Phys. Rev. B **59**, 14177 (1999).
[8] D. Beule *et al.*, Phys. Rev. E **63**, 060202(R) (2001).
[9] V. Celebonović and W. Däppen, Serb. Astron. J. **165**, 23 (2002).
[10] A. M. Lindenberg *et al.*, Phys. Rev. Lett. **84**, 111 (2000).
[11] S. L. Johnson *et al.*, Phys. Rev. Lett. **91**, 157403 (2003).
[12] C. Rose-Petruck *et al.*, Nature (London) **398**, 310 (1999).
[13] C. W. Siders *et al.*, Science **286**, 1340 (1999).
[14] K. Sokolowski-Tinten *et al.*, Nature (London) **422**, 287 (2003).
[15] D. Riley *et al.*, Plasma Phys. Controlled Fusion **47**, B491 (2005).
[16] S. H. Glenzer *et al.* (unpublished).
[17] G. Gregori, S. H. Glenzer, W. Rozmus, R. W. Lee, and O. L. Landen, Phys. Rev. E **67**, 026412 (2003).
[18] J. Chihara, J. Phys. F: Met. Phys. **17**, 295 (1987).
[19] J. Chihara, J. Phys.: Condens. Matter **12**, 231 (2000).
[20] S. Ichimaru, *Basic Principles of Plasma Physics* (Addison, Reading, MA, 1973).
[21] E. E. Salpeter, Phys. Rev. **120**, 1528 (1960).
[22] D. E. Evans and J. Katzenstein, Rep. Prog. Phys. **32**, 207 (1969).
[23] M. W. C. Dharma-Wardana and F. Perrot, Phys. Rev. E **58**, 3705 (1998).
[24] F. Perrot and M. W. C. Dharma-Wardana, Phys. Rev. B **62**, 16536 (2000).
[25] M. W. C. Dharma-Wardana and F. Perrot, Phys. Rev. Lett. **84**, 959 (2000).
[26] N. W. Ashcroft and N. D. Mermin, *Solid State Physics* (Brooks Cole, Monterey, CA, 1976).
[27] D. Bohm and T. Staver, Phys. Rev. **84**, 836 (1951).
[28] E. Flowers and N. Itoh, Astrophys. J. **206**, 218 (1976).
[29] R. M. Housley and F. Hess, Phys. Rev. **146**, 517 (1966).
[30] Y. V. Arkhipov and A. E. Davletov, Phys. Lett. A **247**, 339 (1998).
[31] C. Deutsch, Phys. Lett. **60A**, 317 (1977).
[32] C. Deutsch, M. M. Gombert, and H. Minoo, Phys. Lett. **66A**, 381 (1978).
[33] C. Deutsch, M. M. Gombert, and H. Minoo, Phys. Lett. **72A**, 481 (1981).
[34] P. Seuferling, J. Vogel, and C. Toepffer, Phys. Rev. A **40**, 323 (1989).
[35] R. Kubo, J. Phys. Soc. Jpn. **12**, 570 (1957).
[36] V. V. Belyi, Phys. Rev. Lett. **88**, 255001 (2002).
[37] J. Vogel and C. Toepffer, Phys. Rev. A **43**, 1090 (1991).
[38] L. Pauling and J. Sherman, Z. Kristallogr. **1**, 81 (1932).
[39] D. Pines and D. Bohm, Phys. Rev. **85**, 338 (1952).
[40] D. Pines and P. Nozieres, *The Theory of Quantum Fluids* (Addison-Wesley, Redwood, CA, 1990).
[41] G. Gregori, S. H. Glenzer, and O. L. Landen, J. Phys. A **36**, 5971 (2003).
[42] J. Daligault and M. S. Murillo, J. Phys. A **36**, 6265 (2003).
[43] A. Höll, R. Redmer, G. Röpke, and H. Reinholz, Eur. Phys. J. D **29**, 159 (2004).
[44] H. J. Kunze, in *Plasma Diagnostics*, edited by Lochte-Holgreven (John Wiley & Sons, New York, 1968).
[45] D. A. Baiko *et al.*, Phys. Rev. Lett. **81**, 5556 (1998).
[46] B. E. Warren, *X-Ray Diffraction* (Dover, New York, 1976).
[47] Z. H. Levine and S. G. Louie, Phys. Rev. B **25**, 6310 (1982).
[48] H. Röhr, Z. Phys. **209**, 295 (1968).
[49] H. E. Stanley, *Introduction to Phase Transitions and Critical Phenomena* (Oxford University Press, Oxford, 1971).